A Class of Adaptive Extended State Observers for Nonlinear Disturbed Systems

Zhiqiang Pu, Ruyi Yuan, Jianqiang Yi, *Senior Member, IEEE*, and Xiangmin Tan

***Abstract*—This paper proposes a novel class of adaptive extended state observers (AESOs) that significantly expand the applications of extended state observers (ESOs) to nonlinear disturbed systems. An AESO is designed as a linear time-varying form that, as a result, combines both the advantages of theoretical completeness in a conventional linear ESO (LESO) and good practical performance in a conventional nonlinear ESO (NESO). To tune the time-varying observer gains, AESO error dynamics is first transformed into a canonical (phase-variable) form. Then, time-varying PD-eigenvalues are assigned for the canonical system based on differential algebraic spectral theory. Theorems for stability and estimate error bounds of the AESO are given in the presence of unknown disturbances. These theorems also offer some important guidelines for assigning the PD-eigenvalues. To demonstrate the effectiveness of this new observer, two representative applications, including a numerical single-input–single-output example and a practical multiple-input–multiple-output hypersonic vehicle application, are exemplified, and comparison simulations are conducted among AESO, LESO, and NESO. Future work is pointed out in the end.**

***Index Terms*—Active disturbance rejection control, extended state observer (ESO), PD-eigenvalue, stability analysis, time varying.**

I. Introduction

DISTURBANCES and uncertainties widely exist in almost all physical systems in the real world, in the form of unknown system dynamics or external perturbations. For the control of such systems, a disturbance observer and related techniques have provided a powerful tool to dynamically estimate and compensate the diverse disturbances and offer desired control performances and, thus, have been widely discussed in the literature [1]–[7]. Design of such observers can be pursued by sliding mode [8] or fuzzy [9] techniques. As an alternative, an extended state observer (ESO), which is the centerpiece of the active disturbance rejection control method, was proposed by Han [10]–[12], where all internal and external disturbances were lumped together and represented by an extended state. Thus, both system states and the extended state could be simultaneously estimated. Because of its convenience and high efficiency, the ESO has been widely applied in robotics, aerospace, and electrical machines [13]–[16].

During its rapid development in the last few years, the ESO was split into two typical forms: nonlinear ESO (NESO) and linear ESO (LESO). The NESO was recommended in the early research due to the good estimate efficiency of nonlinear structures. Unfortunately, because of its sophisticated nonlinear structures, rigorous stability derivation for NESO is difficult to be carried out. In the limited literature works, Han utilized both Lyapunov [17] and self-stable region [18] methods to analyze its convergence and estimate errors, but the results were conservative. More generalized convergence results were recently obtained for single-input–single-output (SISO) and multiple-input–multiple-output (MIMO) systems in [19] and [20], respectively. However, many assumptions were made there, and it could be difficult, in practice, to find appropriate nonlinear functions to satisfy these assumptions. For convenience of theoretical analysis, the LESO was developed as an alternative solution, which also displayed simplicity of parameter tuning [21], [22]. However, as reported in [10]–[12], linear structures may not be ideal choices for complicated systems for the loss of design flexibility. In addition, for good performance, the LESO needs larger observer gains, which may go beyond bandwidths of practical systems and, therefore, are physically infeasible. Moreover, a peaking phenomenon may appear in the case of large gains, as in other high-gain observers (see [23, Ch. 14.5]).

Based on the aforementioned analysis, it is intriguing to ask whether a novel observer can be designed, which inherits the advantages and, at the same time, conquers the drawbacks of both NESO and LESO. In this seminal idea, a class of adaptive extended state observers (AESOs) is originally proposed in this paper. AESO is expected to provide more design flexibility and achieve good performance as that in NESO. At the same time, it should have a good form for theoretical analysis, which is a major advantage of LESO. For these purposes, AESO is designed in a linear form with *adaptive* observer gains. Here, the "adaptive" property can be achieved by two approaches: One is to design an adaptive law for the observer gains, as is done in conventional adaptive control; the other is to explicitly assign a time-varying profile for the observer gains. In this paper, the time-varying approach is taken.

With time-varying observer gains, the estimate error system of AESO is cast into a linear time-varying (LTV) system. Thus, in this paper, convergence and estimate errors of AESO are properly analyzed by LTV theories, primarily based on Floquet

Manuscript received October 1, 2014; revised December 29, 2014, March 19, 2015, and May 25, 2015; accepted June 7, 2015. Date of publication June 19, 2015; date of current version August 7, 2015. This work was supported in part by the National Natural Science Foundation of China under Grant 61273149, Grant 61203003, Grant 61421004, and Grant 61403381 and in part by the Special Project for Innovation Methods of MOST under Grant 2012IM010200.

The authors are with the Institute of Automation, Chinese Academy of Sciences, Beijing 100190, China (e-mail: zhiqiang.pu@ia.ac.cn).

Color versions of one or more of the figures in this paper are available online at http://ieeexplore.ieee.org.

Digital Object Identifier 10.1109/TIE.2015.2448060

factorization and differential algebraic spectral theory (DAST) [24]–[28]. By assigning a pertinent time-varying PD-spectrum (a PD-spectrum constitutes a fundamental set of solutions to an LTV system, of which the detailed definition is given in Section III), we cannot only guarantee the convergence of AESO in theory but also flexibly improve its performance according to practical physical constraints and operational conditions. The later aspect is of significant importance in practical applications, particularly when varying system bandwidth (due to varying environment, for example) or constrained energy consumption is taken into consideration.

To sum up, the major contribution of this paper is to propose a novel adaptive ESO that has a better (linear) form than NESO for theoretical analysis and provides better design flexibility and estimate performance than LESO. Stability and estimate error bound are analyzed using DAST. Two representative applications are exemplified to address two possible ways to design the AESO PD-spectrum. This paper is organized as follows. Section II gives a brief statement of conventional NESO and LESO design methods. Section III covers the main research. AESO is constructed, and with a Lyapunov transformation, the AESO error system is transformed into a canonical (phase-variable) form. A time-varying PD-spectrum is assigned for this canonical system to calculate the observer gains. Stability and estimate error bound are analyzed, and results are given in the form of theorems. Advantages of AESO are demonstrated by two examples in Section IV. Conclusion and future work are addressed in Section V.

II. Problem Statement

In this paper, we consider a general n-dimensional nonlinear disturbed system, i.e.,

$$y^{(n)}(t) = f\left(y^{(n-1)}(t), \ldots, y(t), w(t)\right) + b_0 u(t) \tag{1}$$

where $u(t)$ is the single input, $y(t)$ is the single output, b_0 is a given constant, $w(t)$ denotes external disturbance, and $f(y^{(n-1)}(t), \ldots, y(t), w(t))$, or simply denoted as f, represents the nonlinear dynamics of the system, which may contain unknown model information. System (1) is used as mathematical models for a large variety of physical systems. At an extreme, f could be totally unknown. At this point, only the order and the parameter b_0 are given. To tackle this problem, ESO shows unique advantages to dynamically estimate and compensate f with high efficiency. Assume that f is differentiable and denote $\dot{f} = h(y^{(n-1)}(t), \ldots, y(t), w(t))$ with h unknown but bounded. Then, (1) can be rewritten into an extended system, i.e.,

$$\begin{cases} \dot{x}_1 = x_2 \\ \vdots \\ \dot{x}_{n-1} = x_n \\ \dot{x}_n = x_{n+1} + b_0 u \\ \dot{x}_{n+1} = h(x, w) \\ y = x_1 \end{cases} \tag{2}$$

with $x = [x_1, \ldots, x_{n+1}]^T$. We call (2) as the extended system of (1) because the total disturbance f is now taken as an extended state x_{n+1} in (2), which is similar to the "augmented sate" idea in [7]. For (2), an ESO can be constructed, i.e.,

$$\begin{cases} \dot{\hat{x}}_1 = \hat{x}_2 - l_1 g_1(\hat{x}_1 - x_1) \\ \vdots \\ \dot{\hat{x}}_{n-1} = \hat{x}_n - l_{n-1} g_{n-1}(\hat{x}_1 - x_1) \\ \dot{\hat{x}}_n = \hat{x}_{n+1} + b_0 u - l_n g_n(\hat{x}_1 - x_1) \\ \dot{\hat{x}}_{n+1} = -l_{n+1} g_{n+1}(\hat{x}_1 - x_1). \end{cases} \tag{3}$$

Here, $\hat{x}_i$ is the estimate value of x_i, g_i is an appropriately selected function, and $l_i > 0$ is a constant observer gain to be tuned, $i = 1, 2, \ldots, n+1$. By carefully choosing g_i and l_i, one can obtain the estimates of both the original system states and the total disturbance f [10], which could be applied to restructure the system states or construct a dynamical disturbance compensation control law.

The procedure mentioned above addresses the main idea of ESO. In practical applications, with different choices of g_i, (3) is split into two major classes: NESO and LESO. NESO utilizes specific nonlinear function g_i to improve the estimate performance. As originally recommended by Han, g_i is chosen as the following widely used unified nonlinear function with different shaping parameters [10]–[12]:

$$g_i(e_1) = \begin{cases} \frac{e_1}{\sigma_i^{\alpha_i - 1}}, & |e_1| \le \sigma_i \\ |e_1|^{\alpha_i} \operatorname{sign}(e_1), & |e_1| > \sigma_i. \end{cases} \tag{4}$$

Here, $e_1 = \hat{x}_1 - x_1$ is the estimate error of the output x_1, and $\alpha_i \le 1$ and $\sigma_i > 0$ are two shaping parameters of the function. More details on NESO can be found in [10]–[12].

NESO performs well in applications, but its rigorous theoretical derivation, such as its stability and estimate error analyses, is difficult to be carried out due to the sophisticated nonlinear structure. For this reason, LESO was developed, where $g_i(e)$ was trivially chosen as $g_i(e) = e$. In this case, only the constant observer gain l_i needs to be tuned. Gao conducted a complete stability analysis for LESO in [22] and proposed a parameter tuning method in [21] that related the gain l_i to closed-loop bandwidth of the observer; thus, only the bandwidth is needed to be tuned. The readers may refer to [21] and [22] for more details about LESO. However, the choice of linear form for g_i may sacrifice some flexibilities for improving the ESO performance. In addition, large observer gains may go beyond the observer bandwidth and make the required control energy infeasible. For high-gain observers, a peaking phenomenon may occur in the case of a mismatch between the initial true and estimated states (see [23, Ch. 14.5]). To simultaneously inherit the good performance of NESO and the theoretical completeness of LESO, AESO is originally developed in the following section.

III. Design and Stability Analysis of AESO

Go back to the general ESO expression (3). The centerpieces of both NESO and LESO come from constructing specific

function forms of g_i, while the observer gain l_i is set as constant. The novelty of AESO lies in that g_i is still chosen as $g_i(e) = e$, kept in a simple linear form as that in LESO, while the observer gain is set as time varying, that is, $l_i = l_i(t)$, to obtain more design flexibilities. In this seminal idea, AESO is designed in the form of

$$\begin{cases} \dot{\hat{x}}_1 = \hat{x}_2 - l_1(t)(\hat{x}_1 - x_1) \\ \vdots \\ \dot{\hat{x}}_{n-1} = \hat{x}_n - l_{n-1}(t)(\hat{x}_1 - x_1) \\ \dot{\hat{x}}_n = \hat{x}_{n+1} + b_0 u - l_n(t)(\hat{x}_1 - x_1) \\ \dot{\hat{x}}_{n+1} = -l_{n+1}(t)(\hat{x}_1 - x_1). \end{cases} \tag{5}$$

Here, we first transform the estimate error dynamics of AESO (5) into a canonical form that is convenient for theoretical analysis. Then, we give a brief introduction of DAST and, based on that, develop an adaptive method to tune the time-varying observer gain $l_i(t)$. Finally, we conduct a comprehensive analysis of the stability and estimate error bounds of the proposed AESO (5).

A. Transformation of AESO Error Dynamics

In view of (2) and (5), AESO estimate error dynamics can be obtained as

$$\begin{cases} \dot{e}_1 = e_2 - l_1(t)e_1 \\ \vdots \\ \dot{e}_{n-1} = e_n - l_{n-1}(t)e_1 \\ \dot{e}_n = e_{n+1} - l_n(t)e_1 \\ \dot{e}_{n+1} = -l_{n+1}(t)e_1 - h(x,w) \end{cases} \tag{6}$$

or written in a vector differential equation form as

$$\dot{e} = A(t)e + b\,(-h(x,w)) \tag{7}$$

where

$$A(t) = \begin{bmatrix} -l_1(t) & 1 & 0 & \cdots & 0 \\ -l_2(t) & 0 & 1 & \cdots & 0 \\ \vdots & \vdots & \ddots & \ddots & \vdots \\ -l_n(t) & 0 & \cdots & 0 & 1 \\ -l_{n+1}(t) & 0 & \cdots & 0 & 0 \end{bmatrix}, \quad b = \begin{bmatrix} 0 \\ 0 \\ \vdots \\ 0 \\ 1 \end{bmatrix}$$

and $e = [e_1, \ldots, e_{n+1}]^T$, $e_i = \hat{x}_i - x_i$ denoting the estimate error of the ith state, $i = 1, 2, \ldots, n+1$. Obviously, (7) is an LTV system with an unknown but bounded input $-h(x,w)$. In fact, (7) is a canonical form of LTV systems that are uniformly controllable [29]. Next, we need to design proper gain $l_i(t)$ to guarantee the stability of (6) and (7) and, additionally, to obtain good estimate performance. The starting point is to transform (7) into an equivalent canonical (phase-variable) form [30] given below, and the AESO properties will be discussed in the new canonical form. Thus

$$\dot{z} = A_c(t)z + b_c\,(-h(x,w)) \tag{8}$$

where

$$A_c(t) = \begin{bmatrix} 0 & 1 & 0 & \cdots & 0 \\ 0 & 0 & 1 & \cdots & 0 \\ \vdots & \vdots & \ddots & \ddots & \vdots \\ 0 & 0 & \cdots & 0 & 1 \\ -a_1(t) & -a_2(t) & \cdots & -a_n(t) & -a_{n+1}(t) \end{bmatrix}$$

$$b_c = \begin{bmatrix} 0 \\ 0 \\ \vdots \\ 0 \\ 1 \end{bmatrix}.$$

Here, the element $a_i(t)$ is assumed to be smooth (it owns continuous derivatives at any order, if needed in the later derivation) and bounded. Clearly, the canonical form (8) is a realization of the scalar linear differential system, i.e.,

$$\xi^{(n+1)} + a_{n+1}(t)\xi^{(n)} + \cdots + a_2(t)\dot{\xi} + a_1(t)\xi = b_c(-h) \tag{9}$$

where the elements $a_i(t)$ in $A_c(t)$ are directly related to the coefficients of (9). These representations (8) and (9) are central to investigating LTV systems, which will be addressed later. Here, we first discuss how to transform (7) into (8).

The controllability matrix of LTV system (7) is defined as

$$M = [p_1 \;\; p_2 \;\; \cdots \;\; p_{n+1}] \tag{10}$$

where M and p_i, $i = 1, \ldots, n+1$, are, respectively, a square matrix and a column vector of dimension $n+1$, and

$$p_{k+1} = -A(t)p_k + \frac{d}{dt}p_k, \quad p_1 = b,\ k = 1, \ldots, n. \tag{11}$$

The controllability matrix M_c of LTV system (8) is similarly defined. With the definitions (10) and (11), it can be verified by direct construction that

$$M = \begin{bmatrix} 0 & 0 & \cdots & 0 & (-1)^n \\ 0 & 0 & \cdots & (-1)^{n-1} & 0 \\ \vdots & \vdots & \iddots & \vdots & \vdots \\ 0 & (-1)^1 & \cdots & 0 & 0 \\ (-1)^0 & 0 & \cdots & 0 & 0 \end{bmatrix} \tag{12}$$

$$M_c = \begin{bmatrix} 0 & 0 & \cdots & 0 & (-1)^n \\ 0 & 0 & \cdots & (-1)^{n-1} & q_{n,n} \\ \vdots & \vdots & \iddots & \vdots & \vdots \\ 0 & (-1)^1 & \cdots & q_{n-1,2} & q_{n,2} \\ (-1)^0 & q_{1,1} & \cdots & q_{n-1,1} & q_{n,1} \end{bmatrix} \tag{13}$$

where $q_{i,k}$ is defined as in the equation

$$q_{i,k} = \begin{cases} -q_{i-1,k-1} + \dot{q}_{i-1,k}, & 1 < k < i \le n \\ (-1)^{i+1}a_{n-i+2} & \\ \quad + \sum_{j=0}^{i-2} a_{n-j+1}q_{i-1,j+1} + \dot{q}_{i-1,1}, & k = 1 < i \le n \\ (-1)^{i+1}a_{n+1}, & 1 \le k = i \le n. \end{cases}$$

It is seen that the controllability matrix M of the LTV system (7) is constant, whereas the controllability matrix M_c of the

LTV system (8) includes the time-varying element $a_i(t)$ and its derivatives. In addition, from the form of matrices (12) and (13), it is obvious that both (7) and (8) are uniformly controllable. Define $z = T(t)e$, where the transformation matrix $T(t)$ is established as [30]

$$T(t) = M_c(t)M^{-1}(t). \tag{14}$$

Based on the fact that $a_i(t)$ is smooth and bounded, it is easy to verify that $T(t)$ is a Lyapunov transformation [30]–[32] through (12)–(14). That means: 1) $T(t)$ and $\dot{T}(t)$ are continuous; 2) $T(t)$ is nonsingular; and 3) $\|T(t)\|$ and $\|T^{-1}(t)\|$ are bounded. The Lyapunov transformation yields

$$A(t) = T^{-1}(t)\left(A_c(t)T(t) - \dot{T}(t)\right) \tag{15}$$

$$b = T^{-1}(t)b_c. \tag{16}$$

According to (12) and (13), $T(t)$ is calculated as

$$T(t)=\begin{bmatrix} 1 & 0 & \cdots & 0 & 0 \\ (-1)^n q_{n,n} & 1 & \cdots & 0 & 0 \\ \vdots & \vdots & \ddots & \vdots & \vdots \\ (-1)^n q_{n,2} & (-1)^{n-1} q_{n-1,2} & \cdots & 1 & 0 \\ (-1)^n q_{n,1} & (-1)^{n-1} q_{n-1,1} & \cdots & -q_{1,1} & 1 \end{bmatrix}. \tag{17}$$

To obtain the observer gain $l_i(t)$ in (7) through the element $a_i(t)$ in (8), define

$$L(t) = [-l_1(t), \ldots, -l_{n+1}(t)]^T \tag{18}$$

and divide $T(t)$ into $n+1$ columns as

$$T(t) = [T_1(t), \ldots, T_{n+1}(t)] \tag{19}$$

where the column vector $T_i(t) \in \Re^{n+1}$, $i = 1, 2, \ldots, n+1$. Based on (15), the observer gain vector $L(t)$ is calculated as

$$L(t) = T^{-1}(t)\left(A_c(t)T_1(t) - \dot{T}_1(t)\right). \tag{20}$$

Now, we have completed the transformation from (7) to (8) and obtained the calculation formula (20) for the observer gains. For a commonly used second-order AESO (for first-order plants) or third-order AESO (for second-order plants), the transformation matrix $T(t)$ and the observer gains are exemplified as follows.

Example 1: $T(t)$ and the observer gains for a second-order AESO ($n = 1$) are given as

$$T(t) = \begin{bmatrix} 1 & 0 \\ -a_2(t) & 1 \end{bmatrix}, \quad \begin{cases} l_1(t) = a_2(t) \\ l_2 t) = \dot{a}_2(t) + a_1(t). \end{cases} \tag{21}$$

Example 2: $T(t)$ and the observer gains for a third-order AESO ($n = 2$) are given as

$$T(t) = \begin{bmatrix} 1 & 0 & 0 \\ -a_3(t) & 1 & 0 \\ \dot{a}_3(t) + a_3^2(t) - a_2(t) & -a_3(t) & 1 \end{bmatrix},$$
$$\begin{cases} l_1(t) = a_3(t) \\ l_2(t) = a_2(t) - 2\dot{a}_3(t) \\ l_3(t) = a_1(t) + \ddot{a}_3(t) - \dot{a}_2(t). \end{cases} \tag{22}$$

B. Design of $a_i(t)$ Based on DAST

Now that the error dynamics (7) is transformed into the canonical form (8) and the observer gain $l_i(t)$ is expressed by $a_i(t)$ and their derivatives through (20), the successive problem is how to design the time-varying parameters $a_i(t)$ to stabilize AESO and, at the same time, improve its performance as much as possible. In linear time-invariant (LTI) systems, this can be solved as a trivial pole assignment problem. Similar ideas can be extended to LTV systems, but more sophisticated issues should be adequately explored.

In this paper, the time-varying AESO is designed based on DAST. We start with taking the item $b_c(-h(x, w))$ in (8) as a disturbance and considering the homogeneous form for (8) as

$$\dot{z} = A_c(t)z. \tag{23}$$

Similarly, the homogeneous form for (9) is

$$\xi^{(n+1)} + a_{n+1}(t)\xi^{(n)} + \cdots + a_2(t)\dot{\xi} + a_1(t)\xi = 0. \tag{24}$$

As (23) and (24) have identical properties, we proceed by analyzing (24) using DAST. Let $\delta = d/dt$ be the derivative operator, then (24) can be represented as $\mathscr{D}_a\{\xi\} = 0$, where

$$\mathscr{D}_a = \delta^{n+1} + a_{n+1}(t)\delta^n + \cdots + a_2(t)\delta + a_1(t) \tag{25}$$

is the scalar polynomial differential operator (SPDO) for (24). With a Floquet factorization [24], (25) can be written as

$$\mathscr{D}_a = (\delta - \lambda_{n+1}(t)) \cdots (\delta - \lambda_2(t))\,(\delta - \lambda_1(t)) \tag{26}$$

where the definition of $\lambda_i(t)$ and other basic terminologies of DAST are summarized as follows.

Definition 1 [26]:

a) Let $\mathscr{D}_a$ be an SPDO of the scalar differential system (24). Then, the scalar functions $\lambda_i(t)$, $i = 1, \ldots, n+1$, given in (26) are called series D-eigenvalues (SD-eigenvalues) of $\mathscr{D}_a$. Particularly, $\rho(t) = \lambda_1(t)$ is called a parallel D-eigenvalue (PD-eigenvalue) of $\mathscr{D}_a$. Here, $\rho(t)$ is special because $\xi(t) = \exp(\int \rho(t)dt)$ constitutes a solution of $\mathscr{D}_a\{\xi\} = 0$.

b) A multiset $\Gamma_a = \{\lambda_i(t)\}_{i=1}^{n+1}$ with $\lambda_i(t)$ given in (26) is called a series D-spectrum (SD-spectrum) of $\mathscr{D}_a$. A multiset $\Upsilon_a = \{\rho_i(t)\}_{i=1}^{n+1}$ is called a parallel D-spectrum (PD-spectrum) of $\mathscr{D}_a$ if $\rho_i(t)$ are PD-eigenvalues of $\mathscr{D}_a$ and $\{\xi_i(t) = \exp(\int \rho_i(t)dt)\}_{i=1}^{n+1}$ constitutes a fundamental set of solutions to (24).

c) $A_c(t)$ is called the companion matrix associated with $\mathscr{D}_a$. The diagonal matrix $\Upsilon(t) = \mathrm{diag}[\rho_1(t), \ldots, \rho_{n+1}(t)]$ is called a parallel spectral canonical form (PS canonical form) for $\mathscr{D}_a$ and $A_c(t)$.

Based on the definitions above, it shows that when the conventional spectrum concept for LTI systems is extended to LTV systems, it splits into two entities: the SD-spectrum and the PD-spectrum. Either one can characterize system (24) completely. Because PD-eigenvalues are directly related to a set of fundamental solutions to LTV systems, next, we will utilize PD-eigenvalues to investigate (24). An important coordinate

transformation, with transformation matrix $V(t)$, is first made, which reduces the companion matrix $A_c(t)$ to its relevant PS canonical form $\Upsilon(t)$, where

$$\Upsilon(t) = V^{-1}(t)\left[A_c(t)V(t) - \dot{V}(t)\right]. \tag{27}$$

Based on [26], $V(t)$ is calculated as

$$V(t) = \begin{bmatrix} 1 & 1 & \cdots & 1 \\ \mathscr{D}_{\rho_1}\{1\} & \mathscr{D}_{\rho_2}\{1\} & \cdots & \mathscr{D}_{\rho_{n+1}}\{1\} \\ \mathscr{D}^2_{\rho_1}\{1\} & \mathscr{D}^2_{\rho_2}\{1\} & \cdots & \mathscr{D}^2_{\rho_{n+1}}\{1\} \\ \vdots & \vdots & \ddots & \vdots \\ \mathscr{D}^n_{\rho_1}\{1\} & \mathscr{D}^n_{\rho_2}\{1\} & \cdots & \mathscr{D}^n_{\rho_{n+1}}\{1\} \end{bmatrix} \tag{28}$$

where $\mathscr{D}_{\rho_i} = (\delta + \rho_i)$, and $\mathscr{D}^k_{\rho_i} = \mathscr{D}_{\rho_i}\mathscr{D}^{k-1}_{\rho_i}$, $i = 1, \ldots, n+1$, $k = 2, \ldots, n$. It is noted that in an LTI system with distinct eigenvalues, $V(t)$ in (28) coincides with the well-known Vandermonde matrix. Based on (27), the column vectors $v_i(t)$ of $V(t)$ satisfy

$$[A_c(t) - \rho_i(t)I]\, v_i(t) = \dot{v}_i(t) \tag{29}$$

and the row vectors $u_i^T(t)$ of $U(t) = V^{-1}(t)$ satisfy

$$u_i^T(t)\,[A_c(t) - \rho_i(t)I] = -\dot{u}_i^T(t). \tag{30}$$

Thus, $v_i(t)$ and $u_i^T(t)$ are defined as column PD-eigenvectors and row PD-eigenvectors of $\mathscr{D}_a$ associated with $\rho_i(t)$.

To calculate $a_i(t)$ through $\rho_i(t)$, we give the following two lemmas [26] that describe the relationships of $\rho_i(t) \leftrightarrow \lambda_i(t)$ and $\lambda_i(t) \leftrightarrow a_i(t)$, respectively.

Lemma 1: Let $\{\rho_i(t)\}_{i=1}^p$ be a PD-spectrum for a pth-order SPDO $\mathscr{D}_a$ and $V_k(t)$ be the determinant of a kth-order transformation matrix given by (28). Then, the SD-spectrum $\{\lambda_i(t)\}_{i=1}^p$ for $\mathscr{D}_a$ is given by

$$\lambda_k(t) = \rho_k(t) + \dot{V}_k(t)/V_k(t) - \dot{V}_{k-1}(t)/V_{k-1}(t) \tag{31}$$

where $k = 1, \ldots, p$ and $V_0(t) = 1$. ■

Lemma 2: Let $\{\lambda_i(t)\}_{i=1}^p$ be a SD-spectrum for a pth-order SPDO $\mathscr{D}_a$. Define the p coefficients for $\mathscr{D}_a$ as $a_{p,j}(t)$, with $a_{k,0}(t) = 0$ and $a_{k,k+1}(t) = 1$. Then, $a_{p,j}(t)$ can be recursively calculated as

$$a_{p,j}(t) = \dot{a}_{p-1,j}(t) - \lambda_p a_{p-1,j}(t) + a_{p-1,j-1}(t) \tag{32}$$

where $j = 1, \ldots, p$ and $k = 1, \ldots, p-1$. ■

By these two lemmas, we can obtain $a_i(t)$ by assigning appropriate PD-eigenvalues $\rho_i(t)$. This idea is similar to that in LTI systems. However, in LTV systems, the condition that all eigenvalues lie in the left-half plane (LHP) can no longer be a stability criterion. Next, we proceed by investigating the stability and estimate error bounds of AESO, which yields some guidelines to assign the PD-eigenvalues $\rho_i(t)$.

C. Stability and Estimate Error Bound Analysis

Here, we first give a well-known lemma that describes the stability of the homogeneous system (23). Based on this, we analyze the stability and estimate error bounds of the original estimate error system (7).

We first give the following concept of extended mean.

Definition 2 [24]: Let $\eta(t) : I \to \Re$ be a locally integrable function on $I = [t_0, \infty)$. The extended mean of $\eta(t)$ over I is defined as

$$\operatorname{em}(\eta(t)) = \limsup_{T\to\infty} \frac{1}{T} \int_{t_0}^{t_0+T} \eta(t)dt.$$

With Definition 2, the stability of (23) is stated as follows.

Lemma 3 [26]: For (23), let $\Upsilon_a = \{\rho_i(t)\}_{i=1}^{n+1}$ be a PD-spectrum for its associated SPDO $\mathscr{D}_a$, where $\rho_i(t)$ is locally integrable on $I = [t_0, \infty)$. Let $v_i(t)$ and $u_i^T(t)$ be a column PD-eigenvector and a row PD-eigenvector associated with $\rho_i(t)$, respectively. Then, (23) is uniformly exponentially stable on $[t_0, \infty)$ if and only if the following conditions hold.

i) There exists a $0 < m_i \le \infty$ such that

$$\operatorname*{em}_{t\in I}(\operatorname{Re}\rho_i(t)) = -m_i < 0.$$

ii) There exist $k_i > 0$ and $0 < \gamma_i < m_i$ such that

$$\left\|v_i(t)u_i^T(\iota)\right\| < k_i \mathrm{e}^{\gamma_i(t-\iota)}$$

for all $t \ge \iota \ge t_0$.

Furthermore, if (23) is uniformly exponentially stable, its transition matrix $\Phi_z(t, t_0)$ satisfies

$$\|\Phi_z(t, t_0)\| \le k_z \mathrm{e}^{-\gamma_z(t-t_0)}$$

with constants $k_z > 0$ and $\gamma_z = \min\{\vartheta_i\}$, where ϑ_i is defined as

$$\sup(\operatorname{Re}\rho_i(t)) = -\vartheta_i.$$

■

In Lemma 3, the extended mean $\operatorname*{em}_{t\in I}(\operatorname{Re}\rho_i(t))$ is calculated according to Definition 2. It is noted that, compared with the LHP stability criterion in LTI systems, condition (i) requires that all extended means of the PD-eigenvalues should stay in the LHP. That means when some eigenvalues go to the right-half plane for a short time, the system may still stay stable ultimately.

Lemma 3 describes the stability of (23). Next, we give the main results of the stability and estimate error bounds of (7), which, compared with (23), includes both the Lyapunov transformation (15) and the disturbance item $b(-h(x, w))$. The following two lemmas are needed.

Lemma 4 [27]: For an LTV system

$$\dot{\chi} = A_\chi(t)\chi \tag{33}$$

where $A_\chi(t)$ is continuous and bounded, suppose there exists an exponentially stable equilibrium $\chi = 0$. Let $Q(t)$ be a continuous, bounded, positive-definite, and symmetric matrix such that $0 < c_3 I \le Q(t) \le c_4 I$, where I is the identity matrix. Let

$$P(t) = \int_t^\infty \Phi_\chi^T(\tau, t)Q(\tau)\Phi_\chi(\tau, t)d\tau \tag{34}$$

where $\Phi_\chi(\tau,t)$ is the state transition matrix of (33). Then, $P(t)$ is a continuously differentiable, bounded, positive-definite, and symmetric matrix that satisfies

$$-\dot{P}(t)=P(t)A_\chi(t)+A_\chi^T(t)P(t)+Q(t). \tag{35}$$

Hence, $V(t,\chi)=\chi^T(t)P(t)\chi(t)$is a Lyapunov function for (33) that satisfies

$$c_1\|\chi\|^2\le V(t,\chi)\le c_2\|\chi\|^2,$$
$$\dot{V}(t,\chi)\le -c_3\|\chi\|^2,\left\|\frac{\partial V(t,\chi)}{\partial\chi}\right\|\le c_5\|\chi\| \tag{36}$$

where $c_1\sim c_5$ are positive constants, and $c_1=c_3/(2L_\chi)$, $c_2=k_\chi^2c_4/(2\gamma_\chi)$, $c_5=2c_2$. Here, positive constants L_χ, k_χ, and γ_χ satisfy $\|A_\chi(t)\|\le L_\chi$ and $\|\Phi_\chi(t,\tau)\|\le k_\chi e^{-\gamma_\chi(t-\tau)}$. ■

Lemma 5 [23, Lemma 9.2]: Let $\chi=0$ be an exponentially stable equilibrium point of a nominal system $\dot{\chi}=f(t,\chi)$. Let $V(t,\chi)$ be a Lyapunov function of this nominal system that satisfies similar conditions to (36) in $[0,\infty)\times D$, where $D=\{\chi\in\Re^n|\|\chi\|<r\}$. Suppose a perturbed system $\dot{\chi}=f(t,\chi)+g(t,\chi)$ with the perturbation term satisfying

$$\|g(t,\chi)\|\le\delta_f<\frac{c_3}{c_5}\sqrt{\frac{c_1}{c_2}}\theta r \tag{37}$$

for all $t\ge0$, $\chi\in D$, and some positive constant $\theta<1$. Then, for all $\|\chi(t_0)\|<\sqrt{c_1/c_2}r$, the solution $\chi(t)$ of (37) satisfies

$$\begin{cases}\|\chi(t)\|\le ke^{-\gamma(t-t_0)}\|\chi(t_0)\|, & \forall t_0\le t<t_0+t_1\\ \|\chi(t)\|\le b_e, & \forall t\ge t_0+t_1\end{cases}$$

for some finite t_1, where

$$k=\sqrt{\frac{c_2}{c_1}},\quad\gamma=\frac{(1-\theta)c_3}{2c_2},\quad b_e=\frac{c_5}{c_3}\sqrt{\frac{c_2}{c_1}}\frac{\delta_f}{\theta}.$$

■

Based on Lemmas 3–5, we are ready to analyze the stability of (7). The main results are given in the following theorem.

Theorem 1: For the LTV system (7), define a Lyapunov transformation $z=T(t)e$ that transforms (7) into (8). Assume that:

i) the PD-spectrum $\Upsilon_a=\{\rho_i(t)\}_{i=1}^{n+1}$ for the homogeneous system (23) associated with (8) is smooth and bounded, which satisfies the two conditions in Lemma 3.

ii) the disturbance item $b(-h(x,w))$ in (7) satisfies

$$\|b\left(-h(x,w)\right)\|\le\Delta<\frac{c_3}{c_5}\sqrt{\frac{c_1}{c_2}}\theta r$$

for all $t\ge0$, $e\in D$, $D=\{e\in\Re^{n+1}|\|e\|<r\}$ and some positive constants c_1, c_2, c_3, c_5, θ with $\theta<1$.

Then, for all $\|e(t_0)\|<\sqrt{c_1}/c_2r$, the solution of (7) satisfies

$$\begin{cases}\|e(t)\|\le ke^{-\gamma(t-t_0)}\|e(t_0)\|, & \forall t_0\le t<t_0+t_1\\ \|e(t)\|\le b_e, & \forall t\ge t_0+t_1\end{cases}$$

for some finite t_1. The constants used above are calculated as

$$k=\sqrt{\frac{c_2}{c_1}},\quad\gamma=\frac{(1-\theta)c_3}{2c_2},\quad b_e=\frac{c_5}{c_3}\sqrt{\frac{c_2}{c_1}}\frac{\Delta}{\theta}.$$

■

Proof: In view of assumption (i), if the PD-spectrum $\Upsilon_a=\{\rho_i(t)\}_{i=1}^{n+1}$ is chosen to satisfy the two conditions in Lemma 3, the homogeneous system (23) is uniformly exponentially stable, and $z=0$ is an equilibrium. In addition, there exist positive constants $k_z$and γ_z such that the transition matrix $\Phi_z(t,\tau)$ for (23) satisfies $\|\Phi_z(t,\tau)\|\le k_ze^{-\gamma_z(t-\tau)}$ with $\gamma_z=\min\{\vartheta_i\}$, where ϑ_i is defined as $\sup(\mathrm{Re}\rho_i(t))=-\vartheta_i$. As Υ_a is continuous and bounded, the companion matrix $A_c(t)$ is continuous and bounded. From Lemma 4, there exists a positive constant L_z such that $\|A_c(t)\|\le L_z$.

Consider the Lyapunov transformation $z=T(t)e$, which transforms (23) into the homogeneous version of (7), that is,

$$\dot{e}=A(t)e. \tag{38}$$

The transition matrix $\Phi_e(t,\tau)$ for (38) satisfies

$$\Phi_e(t,\tau)=T^{-1}(t)\Phi_z(t,\tau)T(t).$$

As $T(t)$ and $T^{-1}(t)$ are bounded, there exist positive constants k_e and $\gamma_e=\gamma_z$ such that $\|\Phi_e(t,\tau)\|\le k_ee^{-\gamma_e(t-\tau)}$. Therefore, the uniformly exponentially stable property of (23) can guarantee the same property of (38). This coincides with the well-known conclusion that Lyapunov transformation preserves stability [31], [32]. As (38) is uniformly exponentially stable, there exists a positive constant L_e such that $\|A(t)\|\le L_e$.

Let $Q(t)$ be a continuous, bounded, positive-definite, and symmetric matrix. Then, there exist positive c_3 and c_4 such that

$$0<c_3I\le Q(t)\le c_4I$$

then a Lyapunov function $V(t,e)=e^T(t)P(t)e(t)$ for (38) can be constructed, where $P(t)$ is defined as that in (34) and satisfies

$$-\dot{P}(t)=P(t)A(t)+A^T(t)P(t)+Q(t). \tag{39}$$

Following Lemma 4, $V(t,e)$ has the following properties:

$$c_1\|e\|^2\le V(t,e)\le c_2\|e\|^2,\quad\left\|\frac{\partial V(t,e)}{\partial e}\right\|\le c_5\|e\| \tag{40}$$

where $c_1=c_3/(2L_e)$, $c_2=k_e^2c_4/(2\gamma_e)$, and $c_5=2c_2$.

We use $V(t,e)$ as a Lyapunov function candidate for the disturbed system (7). In view of (39) and (40), the derivative of $V(t,e)$ is

$$\begin{aligned}\frac{dV(t,e)}{dt}&=\dot{e}^TP(t)e+e^T\dot{P}(t)e+e^TP(t)\dot{e}\\&=-e^TQ(t)e+2e^TP(t)\left(b\left(-h(x,w)\right)\right)\\&=-e^TQ(t)e+\frac{\partial V(t,e)}{\partial e}\left(b\left(-h(x,w)\right)\right)\\&\le-c_3\|e\|^2+2c_2\|e\|\Delta.\end{aligned}$$

By selecting an appropriate positive constant $0<\theta<1$, we have

$$\begin{aligned}\frac{dV(t,e)}{dt}&\le-(1-\theta)c_3\|e\|^2-\theta c_3\|e\|^2+2c_2\|e\|\Delta\\&\le-(1-\theta)c_3\|e\|^2,\quad\forall\|e(t)\|\ge\frac{2c_2\Delta}{\theta c_3}.\end{aligned}$$

Then, $V(t,e)$ is indeed a Lyapunov function for (7). Based on Lemma 5, we conclude that if the disturbance satisfies

$$\|b\left(-h(x,w)\right)\| \le \Delta < \frac{c_3}{c_5}\sqrt{\frac{c_1}{c_2}}\theta r$$

for all $t \ge 0$, $e \in D$, $D = \{e \in \Re^{n+1} | \|e\| < r\}$, then for all $\|e(t_0)\| < \sqrt{c_1/c_2}r$, the solution $e(t)$ of (7) satisfies

$$\begin{cases} \|e(t)\| \le k\mathrm{e}^{-\gamma(t-t_0)}\|e(t_0)\|, & \forall t_0 \le t < t_0 + t_1 \\ \|e(t)\| \le b_e, & \forall t \ge t_0 + t_1 \end{cases}$$

for some finite t_1. The constants used above are calculated as

$$k = \sqrt{\frac{c_2}{c_1}}, \quad \gamma = \frac{(1-\theta)c_3}{2c_2}, \quad b_e = \frac{c_5}{c_3}\sqrt{\frac{c_2}{c_1}}\frac{\Delta}{\theta}.$$

■

Remark 1: The constants c_1, c_2, and c_5 in Theorem 1 can be calculated by the PD-spectrum-related constants L_e, k_e, and γ_e as $c_1 = (c_3/2L_e)$, $c_2 = (k_e^2 c_4/2\gamma_e)$, and $c_5 = 2c_2$, where $\gamma_e = \gamma_z = \min\{\vartheta_i\}$, $\|A(t)\| \le L_e$. Therefore, we have

$$\|b\left(-h(x,w)\right)\| \le \Delta < \frac{c_3}{c_4}\sqrt{\frac{c_3}{c_4}}\theta r\frac{\gamma_e}{k_e^3}\sqrt{\frac{\gamma_e}{L_e}},$$

$$b_e = \frac{c_4}{c_3}\sqrt{\frac{c_4}{c_3}}\frac{\Delta}{\theta}\frac{k_e^3}{\gamma_e}\sqrt{\frac{L_e}{\gamma_e}}.$$

Here, c_3, c_4, and θ are instrumental variables associated with the Lyapunov stability analysis, whereas L_e, k_e, and γ_e are constants that relate to the PD-spectrum. The disturbance bound $\Delta \propto (\gamma_e/k_e^3)\sqrt{(\gamma_e/L_e)}$, but the ultimate estimate error $b_e \propto 1/((\gamma_e/k_e^3)\sqrt{(\gamma_e/L_e)})$. This offers some guidelines to assign the PD-eigenvalues $\rho_i(t)$. Proper $\rho_i(t)$ cannot only guarantee the stability of AESO (5) but also improve its performance as much as possible, which is the primary advantage of AESO.

Remark 2: In assumption (ii) of Theorem 1, the constant r that determines the definition domain of (7) could be finite or infinite. Accordingly, this assumption requires that the inequality $\|b(-h(x,w))\| \le \Delta < (c_3/c_5)\sqrt{(c_1/c_2)}\theta r$ locally or globally holds. If $r \to \infty$, Theorem 1 states that for all uniformly bounded disturbances, the solution of the perturbed system (7) will be uniformly bounded. The reason for introducing r here is because in most practical applications, the definition domain of e in (7) cannot be infinite due to diverse physical constraints.

IV. Exemplified Applications

ESO has been applied to various fields such as electrical machines, robotics, and aerospace. Clearly, the AESO proposed in this paper can also be similarly applied in these fields, while maintaining better performance than LESO and better form for theoretical analysis than NESO. This section gives two applications to exemplify the design procedure and good properties of AESO. Two different approaches to time-varying PD-eigenvalue design will be separately addressed: In Example 3, it is explicitly designed as a time-based profile; in Example 4, it is determined by dynamic pressure, which is one important environment factor of the system to be controlled.

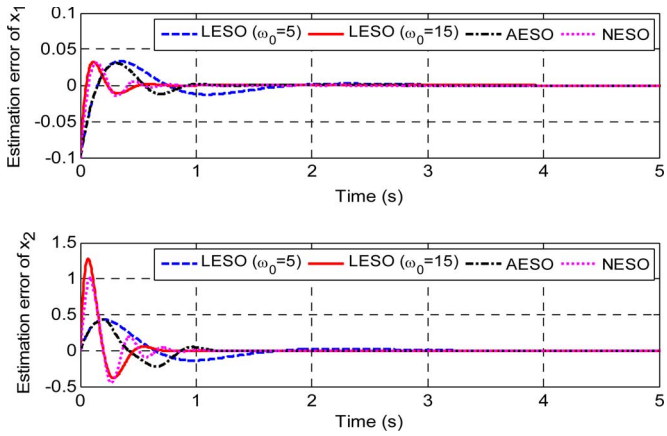

Fig. 1. Estimation error of x_1 and x_2.

Example 3: This example compares the performances of AESO, LESO, and NESO under a mismatch of the initial estimated value; thus, the effectiveness of AESO in suppressing the peaking phenomenon can be exhibited.

Consider a second-order system based on the example given in [23, Sec. 14.5], i.e.,

$$\begin{cases} \dot{x}_1 = x_2 \\ \dot{x}_2 = x_2^3 + u + \Delta \end{cases} \tag{41}$$

where u is the single input, and Δ represents model uncertainty with $\dot{\Delta}$ bounded. Our objective is to estimate both the states and uncertainty to design a compensation control law. Extend the uncertainty as a third state $x_3 = \Delta$. Based on (3), a third-order LESO can be constructed as

$$\begin{cases} \dot{\hat{x}}_1 = \hat{x}_2 - \beta_1 e_1 \\ \dot{\hat{x}}_2 = \hat{x}_2^3 + \hat{x}_3 + u - \beta_2 e_1 \\ \dot{\hat{x}}_3 = -\beta_3 e_1 \end{cases} \tag{42}$$

where $e_1 = \hat{x}_1 - x_1$, $\beta_1 \sim \beta_3 > 0$. Then, a compensation control law, i.e.,

$$u = -\hat{x}_1 - \hat{x}_2 - \hat{x}_2^3 - \hat{x}_3 \tag{43}$$

can be synthesized for closed-loop stability. Assign the constant LESO eigenvalues as $\bar{\rho}_1 = -\omega_0$ and $\bar{\rho}_{2,3} = (-0.5 \pm j0.866)\omega_0$, where $\omega_0 > 0$ represents the observer bandwidth. Then, the observer gains are determined as $\beta_1 = 2\omega_0$, $\beta_2 = 2\omega_0^2$, and $\beta_3 = \omega_0^3$. To improve control performance as much as possible, high observer gains are often used. Here, choose $\omega_0 = 15$ for demonstration. Notice, however, that whenever $x_1(0) \ne \hat{x}_1(0)$, which commonly exists in practice, a peaking phenomenon appears where an impulse response occurs in the estimate errors. Subsequently, there also exists an impulse response in the control variable. In the simulation, set $x_1(0) = 0.1$, $\hat{x}_1(0) = x_2(0) = \hat{x}_2(0) = x_3(0) = \hat{x}_3(0) = 0$, so $x_1(0) \ne \hat{x}_1(0)$. The peaking phenomenon can be seen in Figs. 1 and 2 (solid line), particularly in the estimate errors of x_2 and x_3 and the control u. In practice, the peaking of u may make the control go beyond physical constraints (amplitude or rate, for example) of the actuators and produce an actuator saturation problem. One may reduce the bandwidth ω_0 to attenuate the

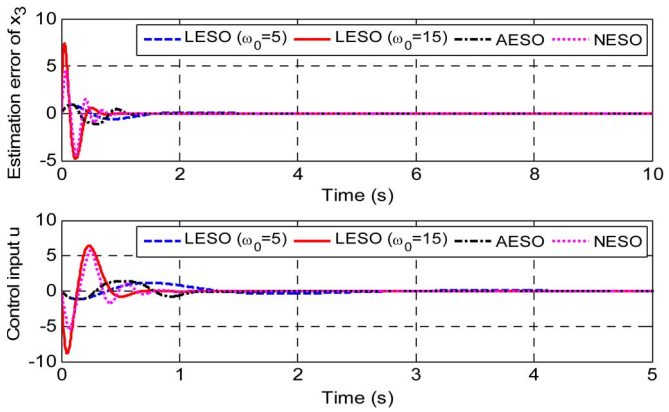

Fig. 2. Uncertainty estimation error and the control input.

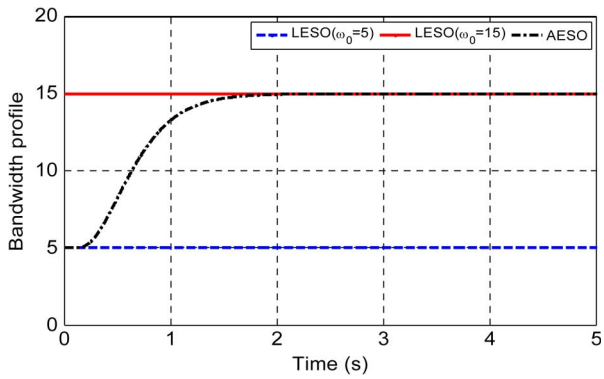

Fig. 3. Bandwidths in the two LESOs and the AESO.

peaking problem. However, as shown in Figs. 1 and 2 (dash-dash line) with $\omega_0 = 5$, the estimation and closed-loop tracking become much slower, and the high-gain observer loses its inherent advantages in terms of "high gain."

Similarly, a third-order NESO can be constructed as

$$\begin{cases} \dot{\hat{x}}_1 = \hat{x}_2 - \beta_1 g_1(e_1) \\ \dot{\hat{x}}_2 = \hat{x}_2^3 + \hat{x}_3 + u - \beta_2 g_2(e_1) \\ \dot{\hat{x}}_3 = -\beta_3 g_3(e_1) \end{cases} \tag{44}$$

where $e_1 = \hat{x}_1 - x_1$, $\beta_1 \sim \beta_3 > 0$. $g_1 \sim g_3$ are selected as the form of (4) with different shaping parameters. Choose the NESO parameters as: $\beta_1 = 20$, $\alpha_1 = 1$, $\sigma_1 = 0.01$; $\beta_2 = 60$, $\alpha_2 = 0.5$, $\sigma_2 = 0.01$; $\beta_3 = 150$, $\alpha_3 = 0.25$, $\sigma_3 = 0.01$. The design of these parameters is based on the parameter tuning principle for ESO given in [12, Ch. 4.8] and empirical trial-and-error tests. This tedious procedure also exhibits a drawback of NESO. Set the initial true and estimated state values the same as those in the LESO above. Since $e_1(0) \neq 0$, the values of the nonlinear functions $g_i(e_1)$ are very large at the beginning. Therefore, peaking also inevitably occurs in NESO, as shown in Figs. 1 and 2 (dot line).

To suppress the peaking appearing in both LESO and NESO, a third-order AESO is designed as

$$\begin{cases} \dot{\hat{x}}_1 = \hat{x}_2 - l_1(t)e_1 \\ \dot{\hat{x}}_2 = \hat{x}_2^3 + \hat{x}_3 + u - l_2(t)e_1 \\ \dot{\hat{x}}_3 = -l_3(t)e_1. \end{cases} \tag{45}$$

To obtain the gains $l_1(t) \sim l_3(t)$, set the eigenvalues as

$$\rho_i(t) = \bar{\rho}_i \omega(t), \qquad i = 1, 2, 3 \tag{46}$$

where $\bar{\rho}_i$ represents "nominal" eigenvalues, and $\omega(t)$ is a time-varying multiplier. Choose the nominal eigenvalues as those in LESO, i.e., $\bar{\rho}_1 = -\omega_0$ and $\bar{\rho}_{2,3} = (-0.5 \pm j0.866)\omega_0$. Then, the time-varying bandwidth of AESO can be obtained as $\omega_n(t) = \omega_0 \omega(t)$. Based on (31) and (32), we have

$$\begin{cases} a_1(t) = -\bar{\rho}_1\bar{\rho}_2\bar{\rho}_3\omega^3(t) \\ a_2(t) = (\bar{\rho}_1\bar{\rho}_2 + \bar{\rho}_1\bar{\rho}_3 + \bar{\rho}_2\bar{\rho}_3)\omega^2(t) \\ \qquad\quad +(\bar{\rho}_1 + \bar{\rho}_2 + \bar{\rho}_3)\dot{\omega}(t) - \ddot{\omega}(t)/\omega(t) + 3\dot{\omega}^2(t)/\omega^2(t) \\ a_3(t) = -(\bar{\rho}_1 + \bar{\rho}_2 + \bar{\rho}_3)\omega(t) - 3\dot{\omega}(t)/\omega(t). \end{cases} \tag{47}$$

Note that, as a special case, if $\omega(t) \equiv 1$, (45) becomes a LESO, and (47) describes the relationship between the roots and coefficients for the relevant characteristic equation. Once $a_i(t)$ is obtained, $l_i(t)$ can be calculated using (22).

The final problem is to design the multiplier $\omega(t)$. Here, we design a time-varying bandwidth profile by explicitly defining a time-based function, i.e.,

$$\omega_{nc}(t) = \begin{cases} 1/3, & t \leq T_\omega \\ 1, & t > T_\omega. \end{cases} \tag{48}$$

$\omega(t)$ and its derivatives in (47) is then generated by a Butterworth filter with $\omega_{nc}(t)$ as the filter input. Equation (48) implies that $\omega_n(t)$ is set as $\omega_0/3$ at the beginning ($t \leq T_\omega$) and increased to ω_0 later ($t > T_\omega$). This logic is helpful in solving the conflict between rapidity and peaking.

Set $T_\omega = 0.2$ s, $\omega_0 = 15$. The AESO-based estimation errors and control input are depicted in Figs. 1 and 2 (dash-dot line). The peaking phenomenon is suppressed in comparison with the LESO ($\omega_0 = 15$) and the NESO, and at the same time, the estimation and tracking are much faster than the LESO with $\omega_0 = 5$. Observer bandwidths in the two LESOs and the AESO are compared in Fig. 3.

Example 4: This example shows a more complicated application where AESO is applied in the attitude control of a winged-cone generic hypersonic vehicle (GHV) [33] for its unpowered decent. The overall control scheme was presented in [34]. In this paper, improvement is made by replacing the disturbance observer there with AESO. As our motivation is to demonstrate the usefulness of AESO in a real MIMO system, here, we just give an outline of the overall control problem, while focus will be placed on AESO design.

The example is to simulate a BTT-180 maneuver during the decent flight of GHV. BTT-180 is an important maneuver particularly for fast entry and landing missions, in which the commanded bank angle is 180°; thus, the lift force turns downward. This maneuver features rapid and wide changes of dynamic pressure, which, in turn, affects the vehicle aerodynamics and behaviors significantly. Before this maneuver, GHV is in a cruise flight condition. The transition from cruise to decent may undergo large initial flight condition dispersion. Thus, in this example, AESO is designed to overcome these two problems:

the varying dynamic pressure and the initial flight condition dispersion.

As presented in [34], the overall attitude control system consists of a slow-state loop (for the angle of attack, bank angle, and sideslip angle dynamics) and a fast-state loop (for the roll rate, pitch rate, and yaw rate dynamics). The controller for each loop is synthesized by combining a basic dynamic inversion control law and an observer-based disturbance compensation law. We consider the fast-state loop here for demonstration, where the motion equations are given as

$$\dot{p} = \left[\bar{L} + (I_y - I_z)qr\right]/I_x \tag{49}$$

$$\dot{q} = \left[\bar{M} + (I_z - I_x)pr\right]/I_y \tag{50}$$

$$\dot{r} = \left[\bar{N} + (I_x - I_y)pq\right]/I_z. \tag{51}$$

Here, I_x, I_y, and I_z are the roll, pitch, and yaw moments of inertia. p,q, and r are the roll, pitch, and yaw rates, which are also the outputs of the fast-state loop. $\bar{L}$, $\bar{M}$, and $\bar{N}$ are the roll, pitch, and yaw moments, which can be approximated by the three control inputs δ_a, δ_e, and δ_r (denoting the deflection angles of right elevon, left elevon, and rudder, respectively, with the amplitude limit as $\pi/6$ rad) as

$$\bar{L} \approx \bar{L}_0 + L_a\delta_a + L_e\delta_e + L_r\delta_r \tag{52}$$

$$\bar{M} \approx \bar{M}_0 + M_a\delta_a + M_e\delta_e + M_r\delta_r \tag{53}$$

$$\bar{N} \approx \bar{N}_0 + N_a\delta_a + N_e\delta_e + N_r\delta_r. \tag{54}$$

Therefore, (49)–(51) can be rewritten as

$$\begin{bmatrix}\dot{p}\\ \dot{q}\\ \dot{r}\end{bmatrix} = \begin{bmatrix}\bar{L}_0 + (I_y - I_z)qr/I_x\\ \bar{M}_0 + (I_z - I_x)pr/I_y\\ \bar{N}_0 + (I_x - I_y)pq/I_z\end{bmatrix} + \begin{bmatrix}L_a & L_e & L_r\\ M_a & M_e & M_r\\ N_a & N_e & N_r\end{bmatrix}\begin{bmatrix}\delta_a\\ \delta_e\\ \delta_r\end{bmatrix}. \tag{55}$$

By introducing a virtual control input, i.e.,

$$U = \begin{bmatrix}U_p\\ U_q\\ U_r\end{bmatrix} = \begin{bmatrix}L_a & L_e & L_r\\ M_a & M_e & M_r\\ N_a & N_e & N_r\end{bmatrix}\begin{bmatrix}\delta_a\\ \delta_e\\ \delta_r\end{bmatrix} \tag{56}$$

the MIMO system (55) can be decomposed into three first-order SISO systems. The coupling effects, along with other uncertainties or disturbances, can be dynamically estimated and compensated by ESO [12]. Here, we investigate the longitudinal pitch rate dynamics for demonstration. Consider that aerodynamic coefficient uncertainty exists in the pitch moment $\bar{M}$, producing an uncertainty item Δ_q. Then, the pitch rate dynamics with uncertainty is written as

$$\dot{q} = f_q + U_q + \Delta_q \tag{57}$$

where $f_q = \bar{M}_0 + (I_z - I_x)pr/I_y$. Similarly to Example 3, a LESO can be constructed to observe the uncertainty, i.e.,

$$\begin{cases}\dot{\hat{x}}_1 = \hat{x}_2 + f_q + U_q - \beta_1 e_1\\ \dot{\hat{x}}_2 = -\beta_2 e_1\end{cases} \tag{58}$$

where $\hat{x}_1$ and $\hat{x}_2$ are, respectively, the estimate of q and Δ_q with $e_1 = \hat{x}_1 - q$. Design the observer gains as $\beta_1 = 2\omega_0$ and $\beta_2 = \omega_0^2$, where the constant bandwidth $\omega_0 > 0$ guarantees the LESO stability.

However, during tuning ω_0, the following two problems occur in view of the varying dynamic pressure and initial flight condition dispersion.

i) At the beginning of the BTT-180 maneuver, ω_0 should be chosen to be relatively small to suppress the peaking phenomenon due to initial condition dispersion.
ii) As the vehicle descends, the dynamic pressure significantly increases due to increasing air density. Consequently, the uncertainty Δ_q becomes larger, and both Δ_q and q change faster. To estimate such variables, ω_0 should be chosen to be relatively large.

To tackle these two problems simultaneously, AESO is a better choice than LESO since it provides a mechanism to flexibly change its bandwidth according to vehicle behaviors and external environment. Design the AESO as

$$\begin{cases}\dot{\hat{x}}_1 = \hat{x}_2 + f_q + U_q - l_1(t)e_1\\ \dot{\hat{x}}_2 = -l_2(t)e_1.\end{cases} \tag{59}$$

For such a second-order system, assign its PD-eigenvalues as [26]

$$\rho_{1,2}(t) = \begin{cases}-\zeta\omega_n(t) \pm j\omega_n(t)\sqrt{1-\zeta^2}, & 0 < |\zeta| < 1\\ -\omega_n(t), -\omega_n(t) + \omega_n(t)\Big/\int \omega_n(t)dt, & |\zeta| = 1\\ -\left(\zeta \pm \sqrt{\zeta^2 - 1}\right)\omega_n(t), & |\zeta| > 1\end{cases} \tag{60}$$

where ζ is a constant damping ratio, and $\omega_n(t)$ is the closed-loop time-varying observer bandwidth. Through (31) and (32), we have

$$a_1(t) = \omega_n^2(t), \quad a_2(t) = 2\zeta\omega_n(t) - \dot{\omega}_n(t)/\omega_n(t). \tag{61}$$

Again, based on (21), the time-varying gains $l_1(t)$ and $l_2(t)$ are expressed by $\omega_n(t)$ as

$$\begin{cases}l_1(t) = 2\zeta\omega_n(t) - \dot{\omega}_n(t)/\omega_n(t)\\ l_2(t) = \omega_n^2(t) + \ddot{\omega}_n(t)/\omega_n(t) - 2\zeta\dot{\omega}_n(t) - \dot{\omega}_n^2(t)/\omega_n^2(t).\end{cases} \tag{62}$$

Note that, as a special case, if $\omega_n(t)$ is set constant, $l_1(t)$ and $l_2(t)$ coincide with the LESO gains β_1 and β_2.

The bandwidth $\omega_n(t)$ and its derivatives $\dot{\omega}_n(t)$ and $\ddot{\omega}_n(t)$ are generated from a third-order Butterworth filter, i.e.,

$$\dddot{\omega}_n(t) + 2\omega_B\ddot{\omega}_n(t) + 2\omega_B^2\dot{\omega}_n(t) + \omega_B^3\omega_n(t) = \omega_B^3\omega_{nc}(t) \tag{63}$$

with its poles assigned at $-\omega_B$ and $(-0.5 \pm j0.866)\omega_B$. This filter determines how $\omega_n(t)$ follows the bandwidth command $\omega_{nc}(t)$. As already pointed out, in BTT-180 maneuver, the vehicle dynamics are significantly affected by the fast time-varying dynamic pressure. A thorough investigation of the relationship between the dynamic pressure and the vehicle states was conducted in [35], where the migration of the poles and zeros for linearized vehicle models was analyzed under different dynamic pressure. Based on this analysis, here,

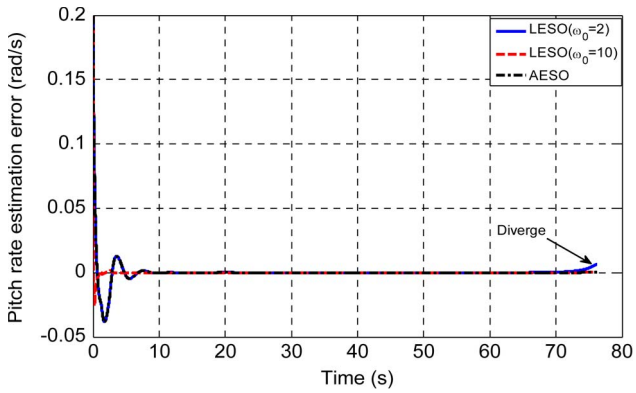

Fig. 4. Comparison of pitch rate estimation error.

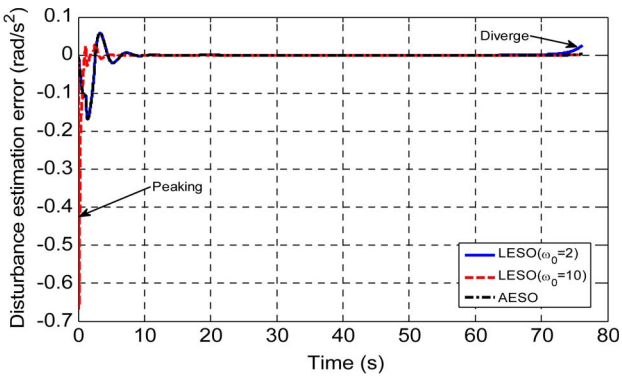

Fig. 5. Comparison of disturbance estimation error.

we design $\omega_{nc}(t)$ as a function of dynamic pressure in the form of

$$\omega_{nc}(t) = sat\left(\omega_{n0}\sqrt{\bar{Q}/\bar{Q}_0}\right). \tag{64}$$

Here, $\bar{Q}$ is the real-time dynamic pressure, $\bar{Q}_0$ is the initial dynamic pressure, and ω_{n0} is the initial AESO bandwidth. The saturation function $sat(\cdot)$ defines the maximum and the minimum of $\omega_{nc}(t)$. ω_{n0} is chosen to be relatively small to overcome the peaking phenomenon at the beginning. As the vehicle descends, $\omega_{nc}(t)$ varies according to the dynamic pressure, which provides better estimation performance under fast varying vehicle behaviors.

Assume that an initial condition dispersion exists where the pitch rate $q(0) = 0 \neq \hat{x}_1(0) = 0.2$. Moreover, add -50% uncertainty to the pitch moment aerodynamic coefficient. Comparison simulation is conducted among two LESOs and one AESO, with $\omega_0 = 2$ and $\omega_0 = 10$, respectively, for the two LESOs and $\zeta = 1$, $\omega_B = 5$, and $\omega_{n0} = 2$ for the AESO. $sat(\cdot)$ constrains $\omega_{nc}(t)$ in the interval [1,10]. Results are depicted in Figs. 4–7. On one hand, under initial condition dispersion, the LESO with a larger bandwidth ($\omega_0 = 10$) exhibits a peaking phenomenon and an actuator saturation at the beginning. On the other hand, as the dynamic pressure increases, the LESO with a smaller bandwidth ($\omega_0 = 2$) exhibits estimation divergence at the late flight stage. However, the AESO performs well through the entire flight stage due to its time-varying parameters shown

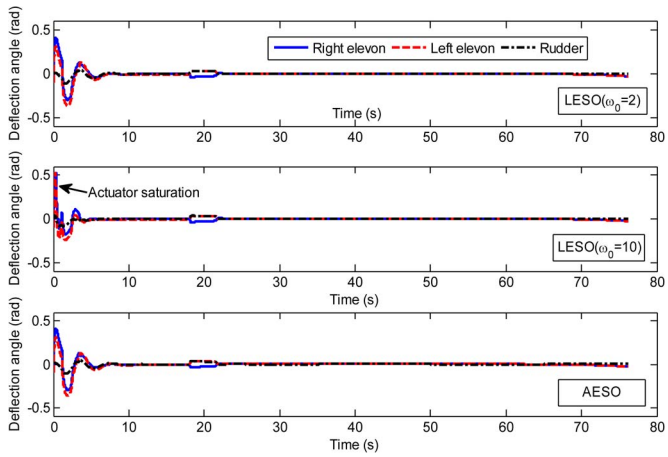

Fig. 6. Comparison of control inputs.

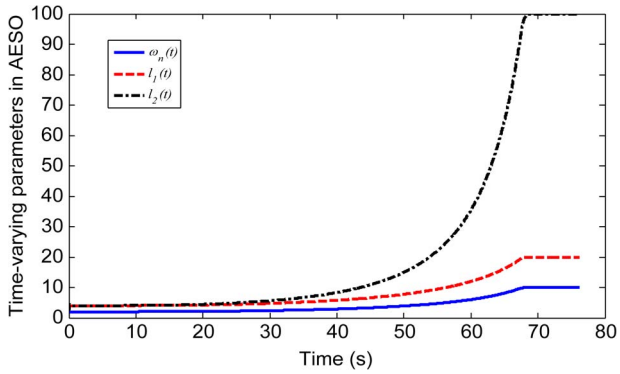

Fig. 7. Time-varying bandwidth and gains for AESO.

in Fig. 7. The bandwidth is small at the beginning and increases in the high-dynamic-pressure regime. Thus, both effects of varying dynamic pressure and initial condition dispersion can be suppressed.

Finally, to verify the robustness of the proposed AESO, measurement noise is considered. Assume that all angular rate measurements are corrupted by Gaussian white noise with mean 0 and covariance 0.0001. This noise is primarily intended to demonstrate the AESO robustness; thus, it is selected to be relatively large. Leave all AESO parameters to be the same as those without measurement noise. Due to page limitations, only the noise and the pitch rate estimation error are depicted in Fig. 8. It is verified that AESO can still work well and the estimation error converges to a small region around zero.

Based on Examples 3 and 4, we finally summarize the design and tuning procedure of an AESO as follows.

Design and Tuning Procedure:

Step 1. Write the AESO in the time-varying form (5).

Step 2. Design time-varying PD-eigenvalue logic according to practical system and environment features. $\rho_i(t)$ can be determined by a time-based profile, an external environment variable, or other vital factors.

Step 3. Tune the eigenvalue $\rho_i(t)$ or relevant bandwidth $\omega_n(t)$. Basically, this relies on specific features of

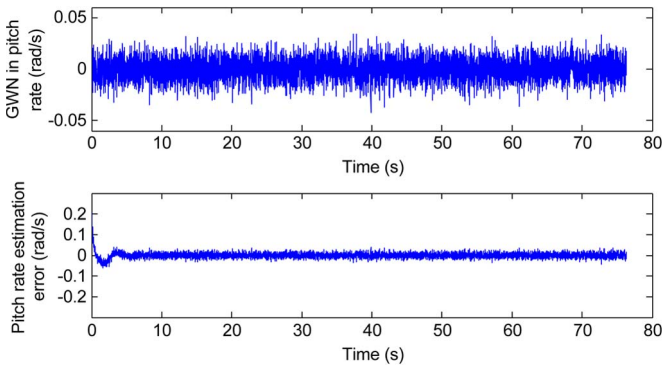

Fig. 8. Robustness verification with measurement noise.

the plant or uncertainty to be observed. However, physical knowledge could be utilized to choose a nominal or an initial bandwidth. Theorem 1 and Remark 1 are also considered to guarantee stability and good performance of the AESO.

Step 4. Calculate the elements $a_i(t)$ of the canonical system (8) through $\rho_i(t)$ according to Lemmas 1 and 2.

Step 5. Calculate the transformation matrix $T(t)$ using (17) and obtain the observer gains $l_i(t)$ through $a_i(t)$ based on (20) [for second-order or third-order AESOs, using (21) or (22)]. This completes the AESO design.

V. Conclusions and Future Work

There always seems to be a conflict between theoretical completeness and practical performance in conventional ESOs, i.e., NESO and LESO. To solve this fundamental problem, this paper has proposed a novel class of adaptive ESOs with time-varying observer gains. As a result, the proposed AESO combines both the advantages of NESO and LESO and provides more extra design flexibility. To tune the time-varying gains, a Lyapunov transformation is first made to transform the AESO error dynamics into a canonical (phase-variable) form. Then, time-varying PD-eigenvalues are assigned based on DAST. Stability and estimate error bounds are subsequently derived, offering some guidelines for assigning the PD-eigenvalues. Finally, two representative examples are conducted, which clearly demonstrate the effectiveness of AESO.

The advantages of the proposed AESO are obvious. For one thing, it has a better (linear) form than NESO for theoretical analysis. Due to its linear form, the notion of bandwidth can be used for parameter tuning. More importantly, stability and estimate error can be analyzed using DAST and other theoretical tools for an LTV system. Moreover, it maintains an adaptive property that can provide better performance than LESO. As a tradeoff, the design of AESO requires better understanding of the overall system features since time-varying eigenvalues are assigned according to practical system characteristics. In addition, parameter tuning may be more complex as the AESO order increases. However, once the order is given, expressions such as (20), (31), and (32) can be given as standard calculation formulas. In future development, more industrial applications and hardware tests will be conducted to validate and improve AESO design. Additionally, some simplifications will be made, on the premise of stability, for high-order observers to produce an easy-designing procedure for practical applications.

References

[1] E. Sariyildiz and K. Ohnishi, "Stability and robustness of disturbance-observer-based motion control systems," *IEEE Trans. Ind. Electron.*, vol. 62, no. 1, pp. 414–422, Jan. 2015.

[2] X. Wang, B. Shirinzadeh, and M. H. Ang, "Nonlinear double-integral observer and application to quadrotor aircraft," *IEEE Trans. Ind. Electron.*, vol. 62, no. 2, pp. 1189–1200, Feb. 2015.

[3] G. Besancon, *Nonlinear observers and applications*. New York, NY, USA: Springer-Verlag, 2007.

[4] D. Ginoya, P. D. Shendge, and S. B. Phadke, "Sliding mode control for mismatched uncertain systems using an extended disturbance observer," *IEEE Trans. Ind. Electron.*, vol. 61, no. 4, pp. 1983–1992, Apr. 2014.

[5] M. Morawiec, "Z-type observer backstepping for induction machines," *IEEE Trans. Ind. Electron.*, vol. 62, no. 4, pp. 2090–2102, Apr. 2015.

[6] T. Nozaki, T. Mizoguchi, and K. Ohnishi, "Decoupling strategy for position and force control based on modal space disturbance observer," *IEEE Trans. Ind. Electron.*, vol. 61, no. 2, pp. 1022–1032, Feb. 2014.

[7] L. B. Freidovich and H. K. Khalil, "Performance recovery of feedback-linearization-based designs," *IEEE Trans. Autom. Control*, vol. 53, no. 10, pp. 2324–2334, Nov. 2008.

[8] Y. Fan, L. Zhang, M. Cheng, and K. T. Chau, "Sensorless SVPWM-FADTC of a new flux-modulated permanent-magnet wheel motor based on a wide-speed sliding mode observer," *IEEE Trans. Ind. Electron.*, vol. 62, no. 5, pp. 3143–3151, May 2015.

[9] X. Ma, Z. Sun, and Y. He, "Analysis and design of fuzzy controller and fuzzy observer," *IEEE Trans. Fuzzy Syst.*, vol. 6, no. 1, pp. 41–51, Feb. 1998.

[10] Z. Gao, Y. Huang, and J. Han, "An alternative paradigm for control system design," in *Proc. 40th Conf. Decision Control*, Orlando, FL, USA, Dec. 2001, pp. 4578–4585.

[11] J. Han, "From PID to active disturbance rejection control," *IEEE Trans. Ind. Electron.*, vol. 56, no. 3, pp. 900–906, Mar. 2009.

[12] J. Han, *Active Disturbance Rejection Control Technique—The Technique for Estimating and Compensating the Uncertainties*. Beijing, China: Nat. Def. Ind. Press, 2009.

[13] S. Li, J. Li, and Y. Mo, "Piezoelectric multimode vibration control for stiffened plate using ADRC-based acceleration compensation," *IEEE Trans. Ind. Electron.*, vol. 61, no. 12, pp. 6892–6902, Dec. 2014.

[14] F. Leonard, A. Martini, and G. Abba, "Robust nonlinear controls of model-scale helicopters under lateral and vertical wind gusts," *IEEE Trans. Control Syst. Technol.*, vol. 20, no. 1, pp. 154–163, Jan. 2012.

[15] J. Yao, Z. Jiao, and D. Ma, "Adaptive robust control of DC motors with extended state observer," *IEEE Trans. Ind. Electron.*, vol. 61, no. 7, pp. 3630–3637, Jul. 2014.

[16] J. Yao, Z. Jiao, and D. Ma, "Extended-state-observer-based output feedback nonlinear robust control of hydraulic systems with back-stepping," *IEEE Trans. Ind. Electron.*, vol. 61, no. 11, pp. 6285–6293, Nov. 2014.

[17] J. Han and R. Zhang, "Error analysis of the second order ESO," *J. Syst. Sci. Math. Sci.*, vol. 19, no. 4, pp. 465–471, Oct. 1999.

[18] Y. Huang, K. Xu, J. Han, and J. Lam, "Flight control design using extended state observer and non-smooth feedback," in *Proc. 40th Conf. Decision Control*, Orlando, FL, USA, Dec. 2001, pp. 223–228.

[19] B. Guo, and Z. Zhao, "On the convergence of an extended state observer for nonlinear systems with uncertainty," *Syst. Control Lett.*, vol. 60, no. 6, pp. 420–430, Jun. 2011.

[20] B. Guo and Z. Zhao, "On convergence of nonlinear extended state observer for multi-input multi-output systems with uncertainty," *IET Control Theory Appl.*, vol. 6, no. 15, pp. 2375–2386, Oct. 2012.

[21] D. Yoo, S. Yau, and Z. Gao, "Optimal fast tracking observer bandwidth of the linear extended state observer," *Int. J. Control*, vol. 80, no. 1, pp. 102–111, Jan. 2007.

[22] Q. Zheng, L. Q. Gao, and Z. Gao, "On stability analysis of active disturbance rejection control for nonlinear time-varying plants with unknown dynamics," in *Proc. 46th Conf. Decision Control*, New Orleans, LA, USA, Dec. 2007, pp. 3501–3506.

[23] H. K. Khalil, *Nonlinear Systems*, 3rd ed. Englewood Cliffs, NJ, USA: Prentice-Hall, 2002, pp. 610–625.

[24] J. Zhu and C. D. Johnson, "Unified canonical forms for matrices over a differential ring," *Linear Algebra Appl.*, vol. 147, pp. 201–248, Mar. 1991.

[25] J. Weon, H. C. Lee, and J. Zhu, "Decoupling and tracking control using eigenstructure assignment for linear time-varying systems," *Int. J. Control*, vol. 74, no. 5, pp. 453–464, Mar. 2001.
[26] J. Zhu, "A unified spectral theory for linear time-varying systems—Progress and challenges," in *Proc. 34th Conf. Decision Control*, New Orleans, LA, USA, Dec. 1995, pp. 2540–2546.
[27] Y. Liu and J. Zhu, "Regular perturbation analysis for trajectory linearization control," in *Proc. Amer. Control Conf.*, New York, NY, USA, Jul. 2007, pp. 3053–3058.
[28] J. Zhu, "Nonlinear tracking and decoupling by trajectory linearization—Lecture note" NASA Marshall Space Flight Center, Washington, DC, USA, 1998.
[29] A. Graham, "A note on a transformation between two canonical forms in state-space in terms of the eigenvalues of the system matrix," *IEEE Trans. Autom. Control*, vol. 13, no. 4, p. 448, Aug. 1968.
[30] L. M. Silverman, "Transformation of time-variable systems to canonical (phase-variable) form," *IEEE Trans. Autom. Control*, vol. 11, no. 2, pp. 300–303, Apr. 1966.
[31] W. A. Wolovich, "On the stabilization of controllable systems," *IEEE Trans. Autom. Control*, vol. 13, no. 5, pp. 569–572, Oct. 1968.
[32] L. A. Zadeh and C. A. Desoer, *Linear System Theory*, New York, NY, USA: McGraw-Hill, 1963, pp. 382–384.
[33] S. Keshmiri, R. Colgren, and M. Mirmirani, "Development of an aerodynamic database for a generic hypersonic air vehicle," presented at the AIAA Guidance, Navigation, and Control Conf. and Exhibit., San Francisco, CA, USA, Aug. 2005, AIAA 2005-6257.
[34] Z. Pu, R. Yuan, X. Tan, and J. Yi, "An integrated approach to hypersonic entry attitude control," *Int. J. Autom. Comput.*, vol. 11, no. 1, pp. 39–50, Feb. 2014.
[35] Z. Pu, R. Yuan, X. Tan, and J. Yi, "Active robust control of uncertainty and flexibility suppression for air-breathing hypersonic vehicles," *Aerosp. Sci. Technol.*, vol. 42, pp. 429–441, Apr./May 2015.

Zhiqiang Pu received the B.Eng. degree in automation control from Wuhan University, Wuhan, China, in 2009 and the Ph.D. degree in control theory and control engineering from the Institute of Automation, Chinese Academy of Sciences, Beijing, China, in 2014.

He is currently a Research Assistant with the Integrated Information System Research Center, Institute of Automation, Chinese Academy of Sciences. His research interests include intelligent robotics, robust control of aerospace systems, and smart devices.

Ruyi Yuan received the B.Eng. degree in communication engineering from Hunan University, Changsha, China, in 2006 and the Ph.D. degree in control theory and control engineering from the Institute of Automation, Chinese Academy of Sciences, Beijing, China, in 2011.

Since 2011, he has been a Research Assistant with the Integrated Information System Research Center, Institute of Automation, Chinese Academy of Sciences. His research interests include control theory and applications, computational intelligence, and unmanned aerial vehicle control.

Jianqiang Yi (M'03–SM'09) received the B.Eng. degree in mechanical engineering from Beijing Institute of Technology, Beijing, China, in 1985 and the M.Eng. and Ph.D. degrees in automation control from Kyushu Institute of Technology, Kitakyushu, Japan, in 1989 and 1992, respectively.

From 1992 to 1994, he was a Research Fellow with the Computer Software Development Company, Tokyo, Japan. During 1994–2001, he was a Chief Engineer with MYCOM, Inc., Kyoto, Japan. Since 2001, he has been a Professor with the Institute of Automation, Chinese Academy of Sciences, Beijing. His research interests include theories and engineering applications of intelligent control, adaptive control, intelligent robotics, and unmanned aerial vehicle systems.

Dr. Yi is an Associate Editor of the *Journal of Advanced Computational Intelligence and Intelligent Informatics* and the *International Journal of Innovative Computing, Information and Control*.

Xiangmin Tan received the B.Eng. degree in automation control from Central South University, Changsha, China, in 2004 and the Ph.D. degree in control theory and control engineering from the Institute of Automation, Chinese Academy of Sciences, Beijing, China, in 2009.

Since 2009, he has been with the Integrated Information System Research Center, Institute of Automation, Chinese Academy of Sciences, where he is currently an Associate Professor. His research interests include advanced robotics, flight control, and vortex jet engine control techniques.